

PYROELECTRIC THIN FILMS INTEGRATED WITH CCD

ALEXANDER SIGOV^a, EUGENY PEVTSOV^a,

ANDREY GORELOV^a, and VLADIMIR CHERNOKOZHIN^b

^aMoscow State Institute of Radioengineering, Electronics & Automation (Technical University),

119454 Moscow, Russia, e-mail: Pevtsov@mirea.ru

^bResearch Institute «PULSAR», 105187 Moscow, Russia

Abstract. We report on fabrication and characterization of three types of pyroelectric thin films: $\text{PbZr}_{0.53}\text{Ti}_{0.47}\text{O}_3$ and BaTiO_3 ceramics, PVDF, and polycyclic organic compound (TADPh). A theoretical model of uncooled focal plane array (UFPA) based on pyroelectric thin film integrated with CCD is proposed. The model of UFPA was designed around the heat balance equations and equivalent circuit. A modified technology of integrated structures of multi-element pyroelectric detectors and special-purpose CCD is proposed. There are designer and manufactured a completely monolithic $100 \times 100 \mu\text{m}^2$ pyroelectric sensor array based on a heat-sensitive film construction lifted slightly above the crystal and also detector specimens with NETD less than 0.2K (8-12 μm at 300 K and 20 Hz). Derived measurements and investigations allowed us to choose the structure of 2D analogue CCD processor integrated with pyroelectric membrane array.

Keywords: pyroelectric thin films; uncooled pyroelectric-CCD sensors

INTRODUCTION

Hybrid package pyroelectric ceramics and CCD was described in Ref.1. Copolymer PVDF can be deposited on CCD readout chip surface through polyimide interlayer [2,3]. In all cases the parameters of such devices were not good enough due to great heat conductivity. A fresh

approach to the problem starts from novel results in MEMS technology [4]. Our attempt to realize a low cost UFPA with complete integration of pyroelectric thin films and CCDs is based just on this approach.

PYROELECTRIC THIN FILMS

We have fabricated and investigated pyroelectric thin films of three types: PZT and BaTiO₃ ceramics, PVDF, and polycyclic organic compound (TADPh).

The Pt/PbZr_{0.53}Ti_{0.47}O₃/Pt/Ti/SiO₂/Si (PZT) and Pt/BaTiO₃/Pt/Ti/SiO₂/Si structures were made by sol-gel routes [5]. The fabrication process involved the following operations: purification, methylcellosolve dehydration, lead trihydrate acetate dehydration, electrochemical operating of zirconium and titanium methylcellosolve solutions followed by preparation of colloids containing all three components. To crystallize the films after polycondensation of metal alcoholates compounds, the oxide layer was subjected to takeout at 600-650°C for 20 minutes.

A 10% solution in methylethylketone was used to make PVDF films. The solution was centrifugally deposited in the solvent vapour on substrates treated by adhesion promoters at fixed process parameters. The films were held at the temperature a bit higher than the melting point and crystallized at fixed temperature for a few hours. Lithography and masked oxygen gas plasmochemical etching were used to form the desired structure on the films. After depositing the top electrode, the PVDF film was polarized at ~200 V/μm field intensity.

The deposition of TADPh films involved two-stage vacuum evaporation. In the first stage a 0.1 μm film was evaporated on the prescreened substrate. The film was then crystallized in organic solvent vapour at 10°C. After crystallization, the properly prepared film was a spheroidal aggregate with preferred orientation. In the second stage a thick layer is deposited on the film.

The layer was also crystallized under slower growth rate conditions. This two-stage evaporation technique permits more homogeneous TADPh films and smaller crystal sizes. The films thus obtained were then dried at about 100° C to remove solvent, and the top electrode was deposited through the mask

Table 1 gives basic physical properties of the films. As seen from the Table, thin pyroelectric films made of different materials and by different methods have comparable figures of merit.

MODEL CALCULATIONS OF INTEGRATED PYROELECTRIC DETECTORS

The calculations are grounded on the principles and assumptions formulated mainly in Refs. [1,4,6,7]. The method proposed for calculating the parameters of multi-element pyroelectric detector with direct injection to the CCD multiplexor is based on solving equations of heat balance and determining signal-to-noise ratio. There are three main factors that play the leading part in design of such devices: temperature transition function of the films under heating by radiation, efficiency of signal charge readout, and noise of pyroelectric detectors and readout IC.

The proposed algorithms of numerical solutions allow us to find with reasonable accuracy the temperature profile for different versions of heat detector constructions. To verify the validity of calculations we compared the results with analytical solutions of corresponding heat balance equations that could be easily obtained for limiting cases. In Fig. 1 there are displayed mean temperature transition functions for different types of construction at 1 K change of scene temperature. As the result, we have found that the values of generalized thermal conductivity of

construction elements of the order of $1\mu\text{W/K}$ could be achieved. The optimum thickness of the film therewith is between 0,5 and 2 μm .

Figure 1. Mean temperature transition functions for different types of detector construction ($1\mu\text{m}$ thick and $\sim 100\times 100\mu\text{m}^2$ area) for different designs: isolated film in vacuum (a); heat sink of $10\mu\text{m}$ diameter in the film centre (b); heat sink along the film perimeter (c); the film on a heat-insulating substrate of polyimide ($10\mu\text{m}$ thick) (d). G_T is heat conductivity of the constructions.

To estimate the efficiency of pyroelectric charge injection into CCD and to calculate signal-to-noise ratio, the equivalent circuit of the whole integrated structure has been analyzed for the case of small signal. The required direct injection of charge can be efficiently (90-95%) provided through the sample intrinsic leakage currents under the applied bias voltage of several volts. The model includes thermal fluctuations of conductivity, dielectric losses, gate leakage noise of input transistor of CCD, noise of the CMOS transistor channel, and flicker noise. The results of calculations for the typical case of the circuit with direct injection are given in Fig. 2. We found that the main noise sources in the given circuit are thermal noise of sensor conductivity and noise of the CMOS transistor channel of CCD input.

Fig. 2. Calculated noise spectral densities and NETD of pyroelectric detector.

For calculations we assumed the following values of parameters of the structure: $2,3\cdot 10^6\text{J/m}^3\cdot\text{K}$ for the specific heat; $3\cdot 10^{10}\text{ Ohm}\cdot\text{m}$ for electric resistivity; 1 pF for readout circuit capacity; $2\mu\text{W/K}$ for total heat conductivity of the construction; $0,13\text{W/m}\cdot\text{K}$ for pyroelectric heat conductivity;

$0,5 \cdot 10^{-4} \text{ C/m}^2 \cdot \text{K}$ for pyroelectric coefficient; $1 \cdot 10^{11} \text{ Ohm}$ for load resistance; $2,63 \text{ W/m}^2 \cdot \text{K}$ for thermal radiation intensity; 0,02 for dielectric loss tangent; 5 for permittivity; $3 \cdot 10^{-16} \text{ A/Hz}^{0,5}$ for spectral density of gate leakage current noise; $1 \cdot 10^{-6} \text{ V/Hz}^{0,5}$ for spectral density of CMOS transistor channel noise. The model demonstrates that optimization of detector design and readout circuit makes it possible to have NETD of about 0,01-0,05 K.

FABRICATION AND INVESTIGATIONS OF PYROELECTRIC-CCD STRUCTURES

In order to achieve high results in designing IR heat detectors, one should make a construction with small thermal mass, suspended by low thermal conductance supports over heat sink. We developed fabrication process of uncooled pyroelectric (PVDF or TADPh) IR sensor isolated from the substrate by air or vacuum gap [7].

As seen in Fig. 3, the photosensitive elements consisting of common top and readout bottom electrodes with a pyroelectric layer in between (this structure also serves as light absorber) are placed on vertical columns. To form the air gap a special buffer repeating the shape of the gap is formed and then removed through the holes in the covering membrane.

Fig. 3 Schematic design of the multi-element integrated detector with polyimide membrane.

In order to investigate the characteristics of array pyroelectric device, the hybrid CCD structure was manufactured. Linear CCD buried-channel low noise multiplexor with direct pyroelectric signal injection was used for these experiments. Experimental measurements allow one to

determine optimum values of signal storage period, modulation frequency, and bias voltage on the pyroelectric capacitor (see, e.g., Fig. 4).

There are designer and manufactured completely monolithic pyroelectric sensor array based on a heat-sensitive film construction lifted slightly above the crystal and also detector specimens (2×128 elements of the area of $100 \times 100 \mu\text{m}^2$) with NETD less than 0.2-0.5 K (for 8-12 μm at 300 K and 20-50 Hz modulation frequency).

Fig. 4. Output CCD signal vs. modulation frequency of incident IR radiation.

The chief and common disadvantage of such detectors, as well as many others, is a nonuniformity of their sensitivity (several tens of percents). One of the ways of mastering this difficulty is the use of electronic correction of the nonuniformity. To find another way, we investigated carefully the pyroelectric coefficient dependence on polarization conditions of thin PZT films [8,9]. These studies, as well as the results of Ref.[10] showed practically linear character of this dependence, on the other hand, a "soft" polarization switch due to polycrystalline structure of ferroelectric thin films is conceivable in this case. Appropriate characteristics were observed under application of symmetric scanning voltage so as under pulse switch of polarization for various amplitudes of switching pulses. Consequently, the field dependence of pyroelectric coefficient permits of corrections of the nonuniformity of film sensitivity.

6. CONCLUSIONS

Starting from preparation and investigation of thin pyroelectric films, we have considered, made, and tested the low-cost device in which thin organic film is integrated with CCD. The technological methods proposed above allow one to prepare integrated structures of multi-element heat detectors and special CCD readout circuits. In thin structure the sensitive film is isolated from the substrate by means of a supporting membrane or serves as the membrane itself. Derived measurements and investigations allowed us to choose the structure of 2D analogue CCD processor which now is under design and which will be integrated with pyroelectric membrane array described above.

ACKNOWLEDGMENTS

This work was supported by Russian Foundation for Basic Research (grant N 01-02-16607), DEFR (project 202.03.01.029), and INTAS (project N01-0075).

References

- [1] R. Watton, P.A. Manning, M.C.J. Perkins, J.P. Gillham, and M.A. Todd: Uncooled IR imaging: hybrid and integrated bolometer arrays. *Proceeding of SPIE*. 1996; 2744: 486-499.
- [2] J. Leconte, R. Barbies, H. Fillon, J.L. Coutures: Pyroelectric mid-resolution camera TH74KB41A. *Proceeding of SPIE*. 1995; 2552: 748-754.
- [3] N. Neumann, R. Kohler, and G. Hofmann: Pyroelectric thin film sensor and arrays based on P(VDF/TrFE). *Integrated Ferroelectrics*. 1995; 6: 213-230.
- [4] P. Muralt: Micromachined infrared detectors based on pyroelectric thin films. *Report on Progress in Physics*. 2001; 64: 1339-1388.
- [5] A.S. Sigov, V.I. Petrovsky, E.Ph. Pevtsov, K.A. Vorotilov, and A.S. Valeev: *Fundamental*

- properties and some applications of sol-gel ceramic thin films. In: Science and Technology of Electroceramic Thin Films: NATO Advanced Research Workshop 20-24 June, 1994, Villa del Mare, Italy. - NATO ASI Series (E); Applied Science, Kluwer Academic Publisher. (Eds. by O. Auciello and R. Waser). Dordrecht, The Netherlands; 1995: 427-437.
- [6] R. Kohler, G. Gerlach, and P. Padmini: Ceramic and polymer thin film in pyroelectric sensors a comparative study. *Journ. of the Korean Physical Society*. 1998; 32: S1744-1746.
- [7] R.W. Whatmore, A. Patel, N.M. Shorrocks, F.W. Ainger: Ferroelectric materials for thermal IR sensors state-of-the-art and perspectives. *Ferroelectrics*. 1990; 104: 269-283.
- [8] V.V. Chernokozin, E.Ph. Pevtsov, M.A.Pospelova, A.S. Sigov: Multi-element uncooled sensors based on organic pyroelectric films integrated with CCD. *Ferroelectrics*. 1999; 225: 67-74.
- [9] V.V. Chernokozin, E.Ph. Pevtsov, A.S. Sigov: Uncooled array IR sensors integrated with CCD analog processor. *Proceedings of SPIE*. 2001; 4761: 98-104.
- [10] M.A. Todd, P.P. Donohue, R. Watton, D.J. Williams, C.J. Anthony, and M.G. Blamire: High performance ferroelectric and magnetoresistive materials for next-generation thermal detector arrays. *Proceeding of SPIE*. 2002; 4795: 88-99.

Figures and table for paper 2481 (A. Sigov)

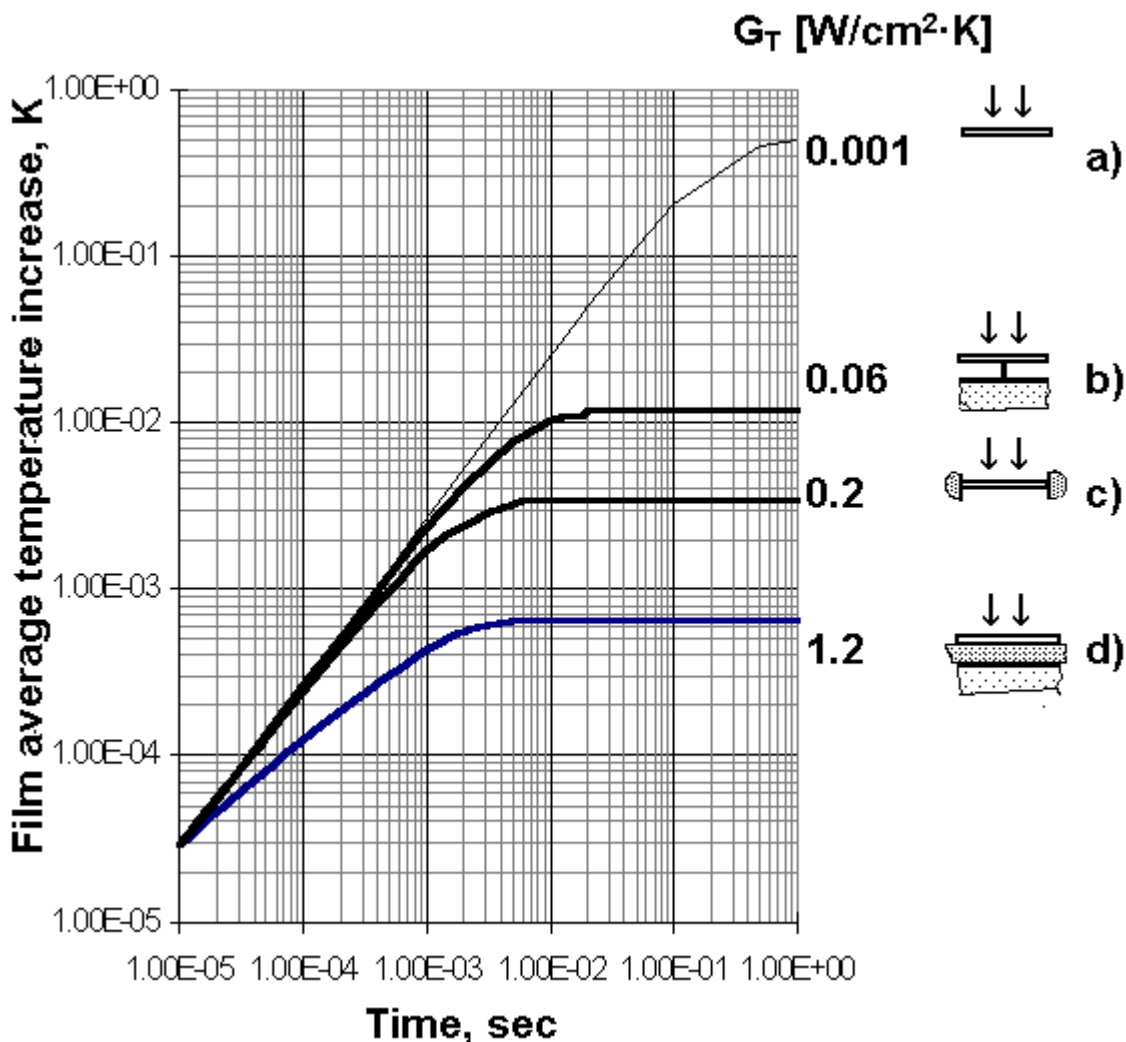


Figure 1. Mean temperature transition functions for different types of detector construction ($1\mu\text{m}$ thick and $\sim 100 \times 100 \mu\text{m}^2$ area) for different designs: isolated film in vacuum (a); heat sink of $10\mu\text{m}$ diameter in the film centre (b); heat sink along the film perimeter (c); the film on a heat-insulating substrate of polyimide ($10\mu\text{m}$ thick) (d). G_T is heat conductivity of the constructions.

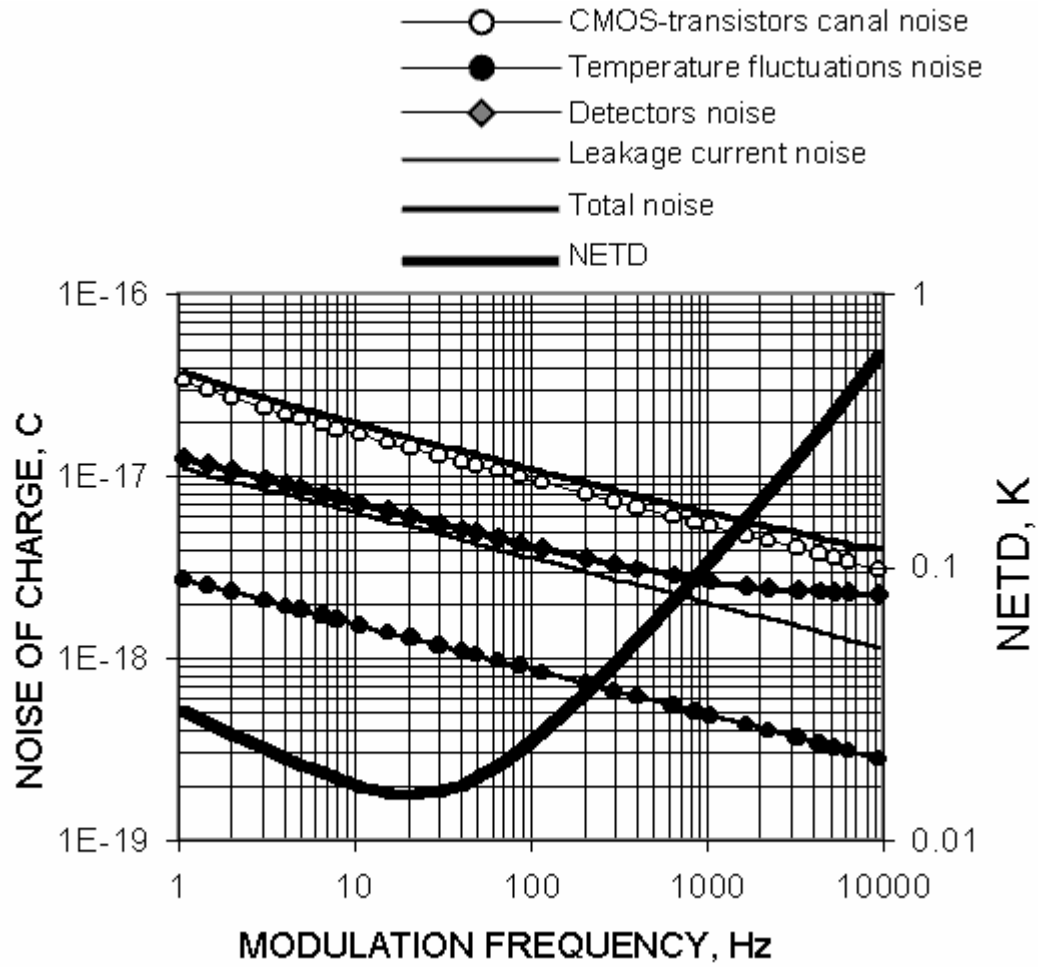


Figure 2. Calculated noise spectral densities and NETD of pyroelectric detector.

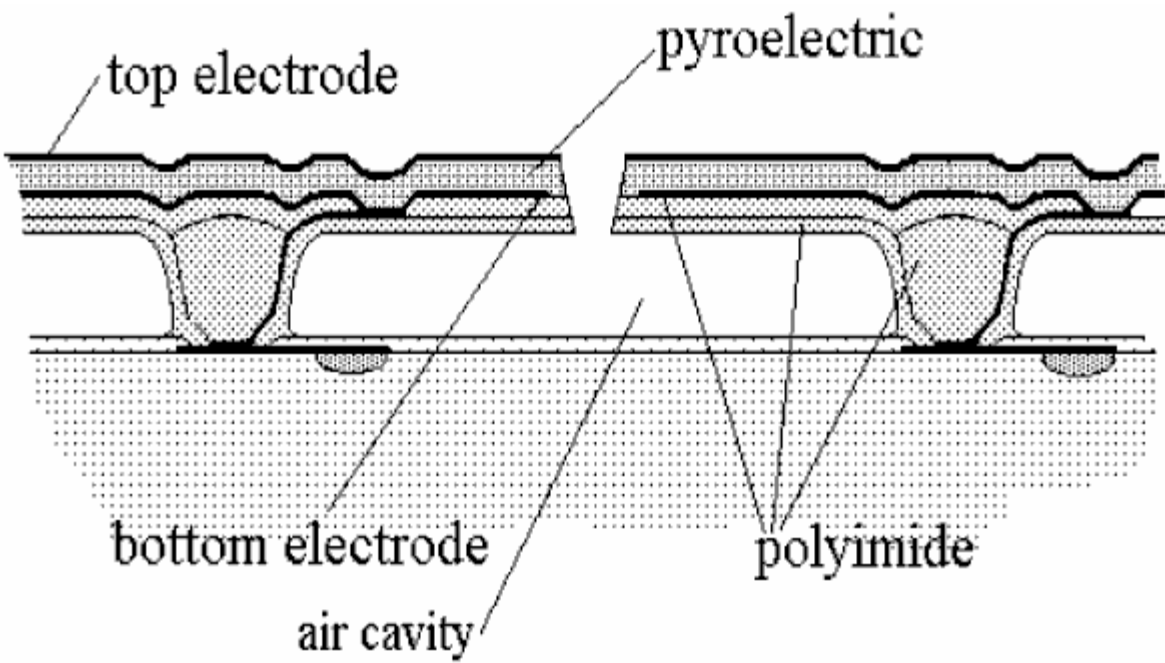


Figure 3. Schematic design of the multi-element integrated detector with polyimide membrane.

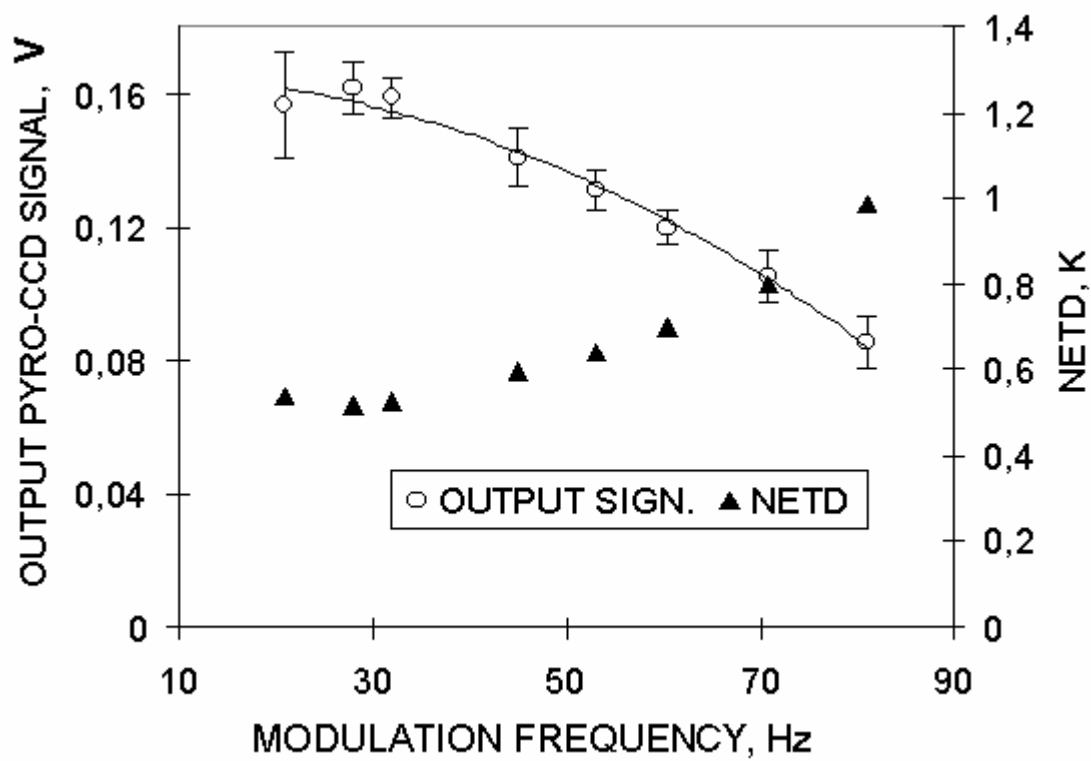


Figure 4. Output CCD signal vs. modulation frequency of incident IR radiation.

Table I. Results of thin films characterization.

Films parameter	PbZr _{0,53} Ti _{0,47} O ₃	BaTiO ₃	PVDF	TADPh
Film thickness, <i>l</i> (μm)	0,2-0,3	0,5-1,0	1,0-1,5	1,0-2,0
Volume specific heat, <i>c_v</i> , (J/cm ³ ·K)	2,7	2,5	2,3	1,8
Pyroelectric coefficient, <i>p</i> (nC/cm ² ·K)	20	10	3,1	5,1
Permittivity, <i>ε</i> (0V, 100 Hz)	500	140	9	4
Dielectric loss, <i>tan δ</i> (0V, 100 Hz)	0,008	0,012	0,015	0,023
Figure of merit, <i>F_D</i> = <i>p</i> /(<i>c_v</i> (<i>εε₀tan δ</i>) ^{0,5}) (10 ⁻⁵ Pa ^{-0,5})	3,1	3,3	1,1	1,4